Available online at www.sciencedirect.com
SCIENCE DIRECT®
Journal of the European Ceramic Society 25 (2005) 695–702
www.elsevier.com/locate/jeurceramsoc

Aluminothermic reduction of zirconia

Xiaoli Zhe, C. A. Dioka, A. Hendry

Materials & Metallurgy Group, Department of Mechanical Engineering, University of Strathclyde, 75 Montrose Street, Glasgow, Scotland G1 1XJ, UK

Received 10 October 2003; received in revised form 26 November 2003; accepted 7 December 2003

Available online 17 June 2004

Abstract

Results are presented for the reaction of aluminium metal with zirconia ceramics under (reducing) sintering conditions. During hot-pressing the principal phase formed is zirconium monoxide which is shown to have a rock-salt cubic structure and a unit-cell dimension of 0.46258 nm. When pressureless sintered or hot-pressed using a yttria partially-stabilised zirconia, composite structures of ZrO, alumina and cubic zirconia are produced which are the result of reduction reactions which proceed through the liquid metal phase. The results are interpreted through X-ray diffraction, microstructural and phase equilibria considerations which show that the sintering gas also plays a role in reaction through the oxygen partial pressure.

The results allow calculation of an approximate value of the free energy of formation of zirconium monoxide ($-294{,}500\,\mathrm{J\,mol^{-1}}$) which is consistent with the reported values for the monatomic carbide and nitride of zirconium and with other similar transition metal carbide, nitride and monoxide series.

Keywords: ZrO; ZrO_2; Hot-pressing; X-ray methods; Free energy of formation

1. Introduction

Cubic zirconium dioxide is known to be an oxygen ion conductor[1] and an important phase in toughenable cubic/tetragonal partially-stabilised zirconia structural ceramics.[2] Thus, there are features of the behaviour of zirconia which are important in both functional and structural ceramic applications. In addition, zirconia is also used as a corrosion-resistant high-temperature material in slag-band inserts in submerged entry refractory tubes in one continuous casting of steel.[3] The technology of zirconia is well understood in each of those respects but the development of specific properties depends on the processing route and in many cases these are complex and expensive. There is a need therefore to develop for industrial ceramics new methods of producing tailored zirconia microstructures which do not require high-cost materials or complex production routes. This applies in particular to zirconia for functional use. The present work describes the development of such materials and microstructures for sensor applications.

The origins of the present paper lie in the application of self-sustaining high-temperature synthesis (SHS) in the form of aluminothermic reduction to the formation of controlled morphology zirconia composites. Previous work has shown[4,5] that a simple approach of powder processing and control of ceramic/gas interaction on sintering can produce microstructures with combinations of functional properties and good high-temperature mechanical strength.

The technological applications are speculative but the preliminary work[6] has shown that microstructures which can be used as sensors are possible. For example, in nitride-bonded silicon carbide tubes for combustion an insert of the appropriate zirconia composite with ionic oxygen-conducting character could be used as the electrolyte to monitor combustion conditions inside the tube. The material has sufficiently good strength and is resistant to thermal shock but can also be incorporated into the tube structure by conventional isostatic pressing and firing during which the aluminothermic reduction forms the required microstructure in situ. However, before any such applications can be considered a full knowledge of the parameters controlling the development of microstructure must be established.

The present paper addresses several of the relevant parameters and a combination of physical examination and analysis

0955-2219/$ – see front matter © 2004 Elsevier Ltd. All rights reserved.
doi:10.1016/j.jeurceramsoc.2003.12.033

techniques has been used to clarify the stages of microstructural development during the aluminothermic reduction of zirconia. From these results conclusions are drawn regarding the mechanisms which prevail and which can then be employed to develop controlled processing routes for manufacture.

2. Experimental procedure

To produce a highly reduced zirconium oxide, commercial aluminium powder (Goodfellow Metals) with mean particle size of 30 μm and purity 99.9% and tetragonal yttria-stabilised zirconia powder (Zirconia Sales U.K., Ltd.) with mean particle size of 0.5 μm and purity 99.7% were used as reactants. Up to 20 wt.% (53.9 mol%) of commercial aluminium was mixed with 80 wt.% Y-stabilised zirconia powder (Table 1) and ball milled with alumina balls and alcohol in a propylene jar for one hour. The dried mixture was isostatically compressed for sintering at pressure of 350 MPa into pellets of diameter 20 mm and thickness 5 mm. Sintering was carried out in a carbolite tubular furnace sealed at both ends, with orifices for the passage of gas. Dry argon gas was continuously pumped through the furnace heating chamber throughout the sintering process. Sintering was done at 1400 °C for 1 h at a heating and cooling rate of 5°/min, respectively.

Control samples of aluminium with pure monoclinic zirconia were prepared in a similar manner.

Hot-press sintering (HP) was conducted in air using an induction heated facility with graphite tooling. A boron nitride (BN) powder bed was employed to prevent direct reaction between the green pellet and the graphite die in a standard hot-pressing assembly and this arrangement also provides a quasi-isostatic pressure during hot-pressing. The temperature was controlled manually and monitored by an optical pyrometer. The reading taken from the surface of the graphite die was corrected to a real temperature inside the die with accuracy of ±10 °C. After heating to sintering temperatures within 0.5 h, samples were held for 0.5 h under a quasi-isostatic pressure of 70 bar and then cooled to below 1000 °C in 0.5 h with the pressure removed.

X-ray diffraction data were obtained using a Philips step-scanning diffractometer with Cu Kα radiation and a Ni filter using a step size of 0.1° and a counting time of 20 s. The microstructure of the composite was examined using a CAMECA SX100 electron-probe micro-analyser (EMPA) with EDS (energy dispersive spectroscopy) and WDS (wavelength dispersive spectroscopy) capability for the light elements O, N and C.

Table 1
Compositions

Powder	Additive	ZrO_2	Phase
(a) Composition and phase of powders (mol%)			
ZrO_2	–	>99.8	Monoclinic
Y-ZrO_2	$3Y_2O_3$	97	Tetragonal
Sample	Al-metal	Ceramic	
(b) Starting composition of composites (wt.%)			
20Z	20	80 ZrO_2	
5Y	5	95 Y-ZrO_2	
10Y	10	90 Y-ZrO_2	
20Y	20	80 Y+-ZrO_2	

3. Results

3.1. General view of phases in the composites

X-ray diffraction results (XRD) of sample 20Z hot-pressed between 1000 and 1500 °C for 0.5 h, show that the only Al-containing compound is α-Al_2O_3 and no metallic Al can be detected in the sample. This clearly indicates that Al reacted totally to form alumina during sintering. Fig. 1 is a representative XRD pattern of a sample hot-pressed at 1500 °C. There are two modifications of zirconia present, monoclinic and cubic phases. The former is possibly untransformed zirconia from the starting materials but the latter is unusual in that the cubic phase does not usually occur in a sintered sample without a stabilising oxide additive (as discussed later). The major phase, however (marked by ∇) is the most interesting component in the specimen. Structurally, it is similar to ZrC and ZrN in the intensity of the peaks which are characteristic of a rock-salt structure but different from the latter in cell dimension, which is close to ZrO(s). To identify this ZrO-like phase, a more precise diffraction pattern with scan step of 0.01° and internal standard KCl was taken from the same specimen for further indexing of reflections and refinement of the lattice constant.

3.2. Indexing and refinement of cell dimensions for the ZrO-like phase

The corrected peak positions with accuracy better than 0.02° from specimens of 20Z were used to carry out indexing and refinement of the lattice constant. The result with a figure of merit of 125 (very good refinement) is shown in Table 2. The refined cubic unit-cell of $a = 0.46258$ nm is significantly different from 0.4577 nm for ZrN and 0.4693 nm for ZrC (ICDD cards 35-753 and 35-784). The difference is too large to be considered as an error in the X-ray experiment. A similar result was obtained ($a = 0.46289$ nm) for this specimen by a Hagg–Guinier camera technique.[7] The only similar literature evidence of a rock-salt structure is zirconium monoxide ZrO, reported as a calculated pattern with $a = 0.4620$ nm in ICDD card 20-684. This substance was generally believed not to be stable as a pure solid phase.[8]

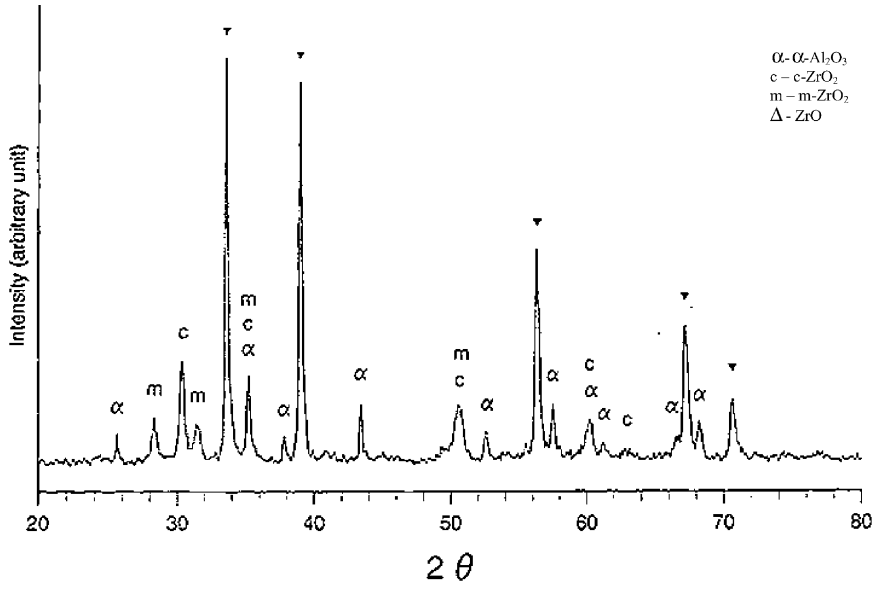

Fig. 1. XRD pattern of composite sample 20Z hot-pressed at 1500 °C.

Table 2
Refined unit-cell parameters and diffraction data of the major Zr-containing phase in a sample of 20Z hot-pressed at 1500 °C

h	*k*	*l*	2θ observed	2θ calculated	I_{obs}	d_{obs}
1	1	1	33.530	33.528	100	2.6705
2	0	0	38.904	38.908	91	2.3131
2	2	0	56.214	56.198	48	1.6350
3	1	1	67.064	67.049	35	1.3945
2	2	2	70.464	70.459	13	1.3353
4	0	0	83.524	83.533	9	1.1565
3	3	1	93.090	93.081	12	1.0611
4	2	0	96.294	96.269	18	1.0342
4	2	2	109.296	109.332	14	0.9444

a=0.46258 m; S.G.: *Fm*3*m* (2 2 5).

3.3. Phases in Y-stabilised zirconia composites

Phases in 20 wt.% Al–Y/ZrO_2 hot-pressed at 1500 °C are shown by XRD in Fig. 2. The major phase is again a ZrO-like compound with cell dimension of 0.46250 nm. It slightly differs from that in 20Z sintered at the same temperature. The only Al-containing phase is α-Al_2O_3 and no Y-Al garnet was found in the samples contrary to what was expected. This indicates that yttria is still in solid solution in the ZrO_2 phase as a stabiliser. Comparing with the tetragonal ZrO_2 in the starting materials, there is only the cubic modification of ZrO_2 after sintering.

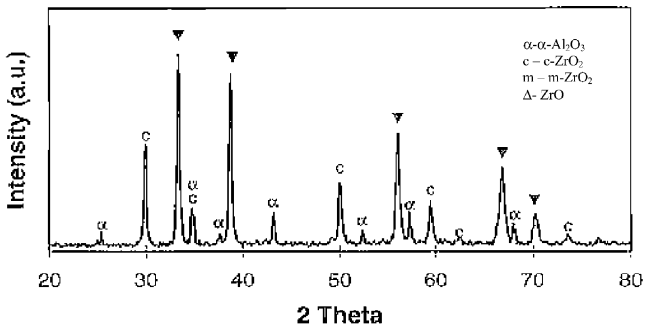

Fig. 2. XRD pattern of composite sample 20Y hot-pressed at 1500 °C.

For different amounts of Al additive, the composition of phases of Y-stabilised zirconia composites hot-pressed at 1400 and 1500 °C is shown in Table 3. In contrast to composites with pure zirconia, there is a strong tendency to form cubic ZrO_2 even at lower temperature. The ZrO-like phase is not formed in conditions where temperature is <1400 °C and Al additive is <10 wt.%.

3.4. Pressureless sintering of Y-stabilised zirconia composites

Fig. 3 shows the X-ray pattern of a sample containing 20%Al which has been pressureless sintered in argon for 1 h at 1400 °C. When compared with Fig. 2 it is clear that there are significant differences from the phase distribution after hot-pressing. The amount of the rock-salt phase is considerably smaller while the proportion of cubic zirconia has increased and a small amount of monoclinic zirconia is present. Most significantly, however, is the presence of a small amount of yttrium aluminium garnet which although

Table 3
Phases in Y-composites hot-pressed at 1400 and 1500 °C

Temperature (°C)	5Y	10Y	20Y
1400	c + α	c + α	c + ∇ + α
1500	c + α	c + ∇ + α	∇ + c + α

Note: ∇, ZrO-like; c, c-ZrO_2; m, m-ZrO_2 and α, α-Al_2O_3; appear in high to low sequence against the most intensive peak in each phase.

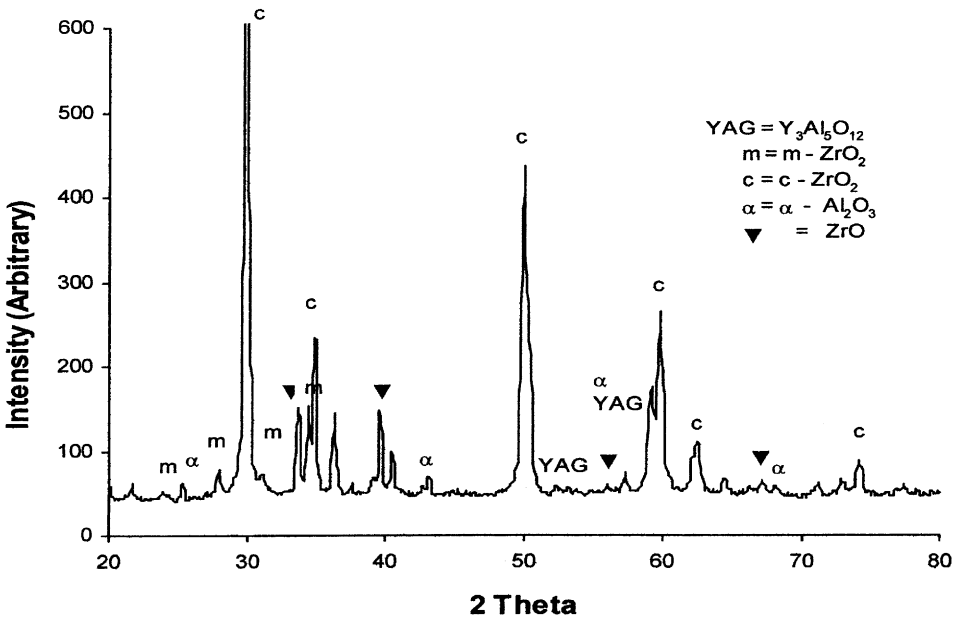

Fig. 3. XRD pattern of composite sample 20Y sintered at 1400 °C.

expected from these reactions was not present in any of the hot-pressed samples.

3.5. Microstructure

An optical micrograph of the general appearance of the sintered composites is shown in Fig. 4. This appearance is typical of both hot-pressed and of pressureless sintered samples and shows roughly spherical regions which reflect the shape and size of the original aluminium metal particles which have subsequently melted and reacted during sintering. Within these regions there is finer microstructural detail which is discussed below. The matrix is typical of sintered zirconia with a relatively fine grain structure and considerable porosity.

EPMA data in the form of area plots have been used to identify the elemental distribution in the microstructure. Fig. 5 shows elemental maps of the distribution of Al, Zr and O in the reacted metallic particles. It is clear that zirconium and oxygen have been incorporated into the aluminium metal resulting in a eutectic-like structure of mixed zirconium and aluminium oxides and with a region around the outer periphery which is high in alumina and lower in zirconia.

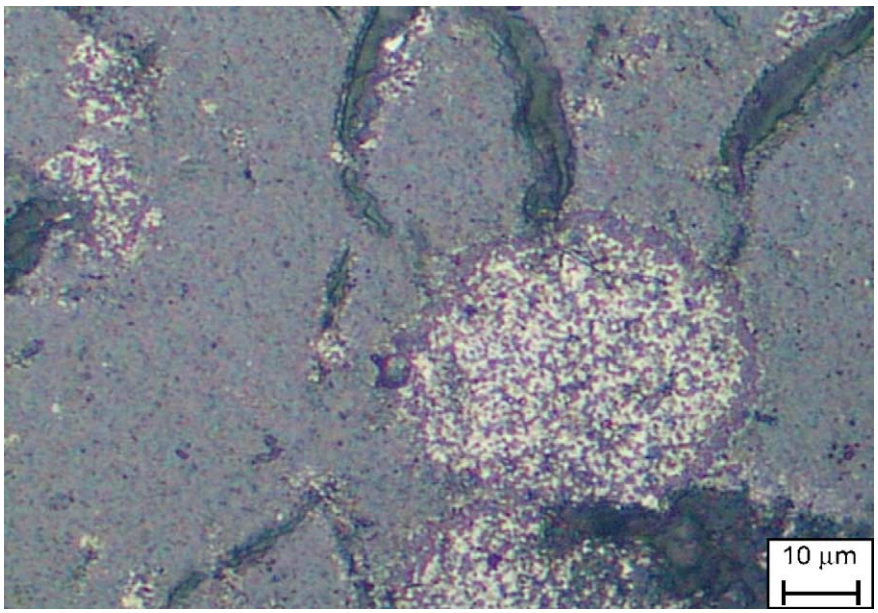

Fig. 4. Optical micrograph of a reacted aluminium particle in the zirconia matrix (sintered at 1400 °C).

4. Discussion

It is clear from the results of X-ray diffraction studies that the phases formed by aluminothermic reduction of zirconia depends on both the nature (stabilised or pure material) of the zirconia used and the conditions of sintering. In the absence of a stabilising additive (ytrria) the product of reaction hot-pressing is primarily the ZrO rock-salt phase with some residual monoclinic zirconia from the starting material and also some cubic zirconia. All of the aluminium metal has been converted to aluminia. When yttria-stabilised zirconia is used the composition after hot-pressing is similar but no monoclinic zirconia is present indicating that additional stabilisation by yttria has produced only cubic zirconia. In the case of pressureless reaction sintering the proportion of phases is different (Fig. 3) with a much lower proportion of the ZrO phase as a result of the less strongly reducing conditions when compared to hot-pressing. In all cases, however, the microstructure is “composite”; that is it is a heterogeneous distribution of phases.

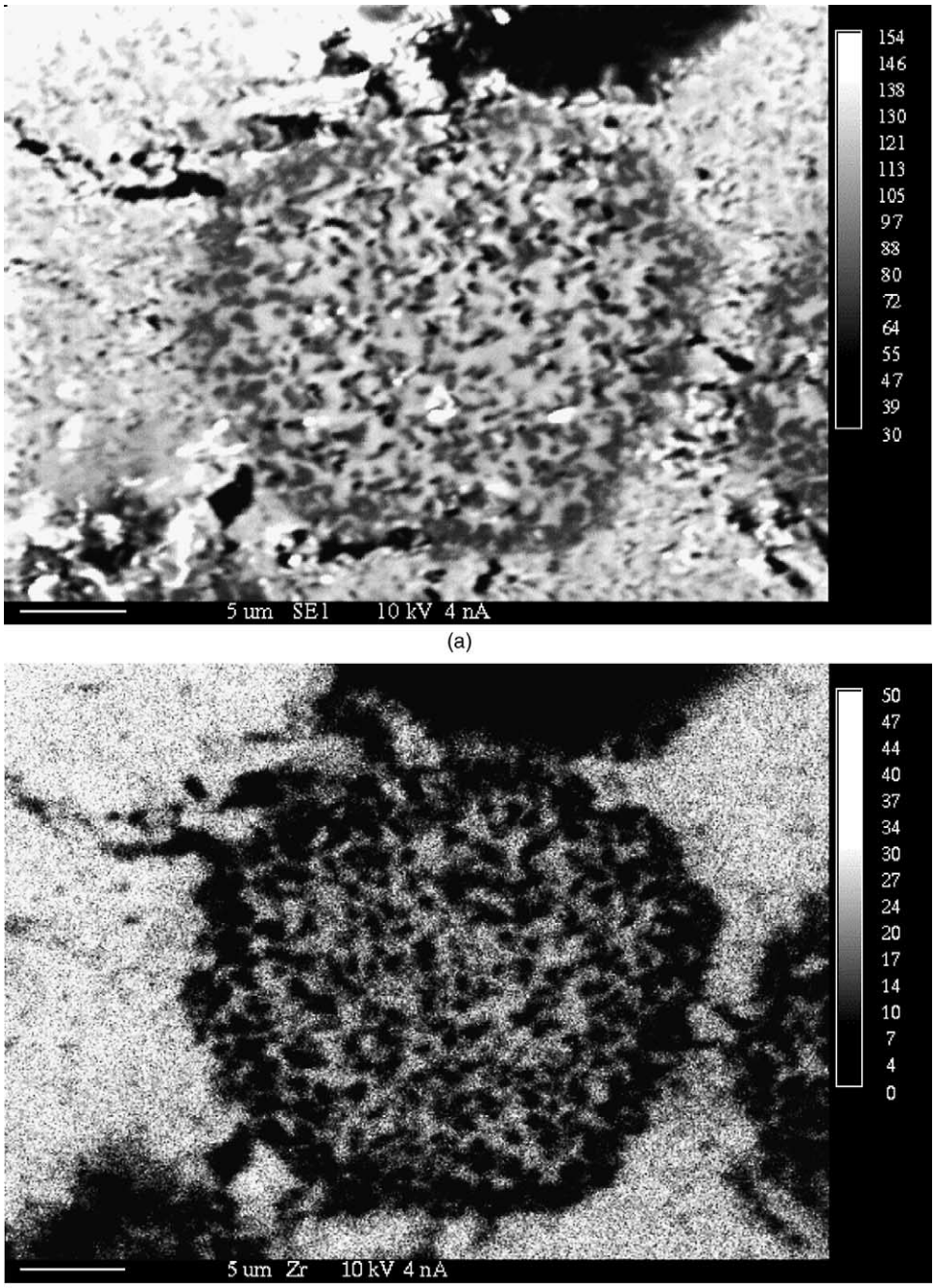

Fig. 5. (a) Secondary electron image of the sample in Fig. 4. (b) EPMA zirconium concentration map as in (a). (c) EPMA oxygen concentration map as in (a). (d) EPMA aluminium concentration map as in (a).

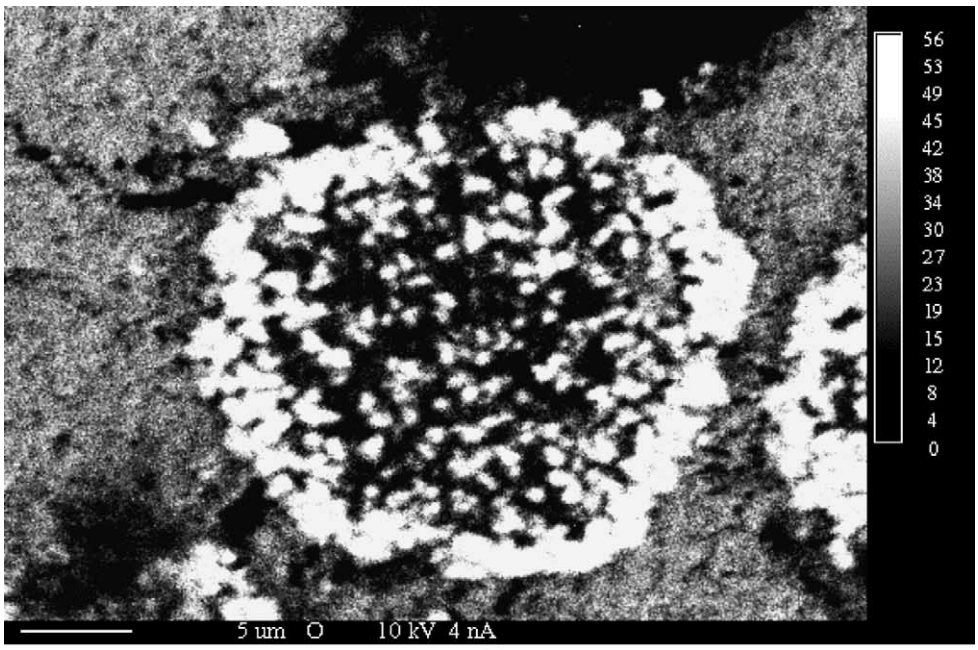

(c)

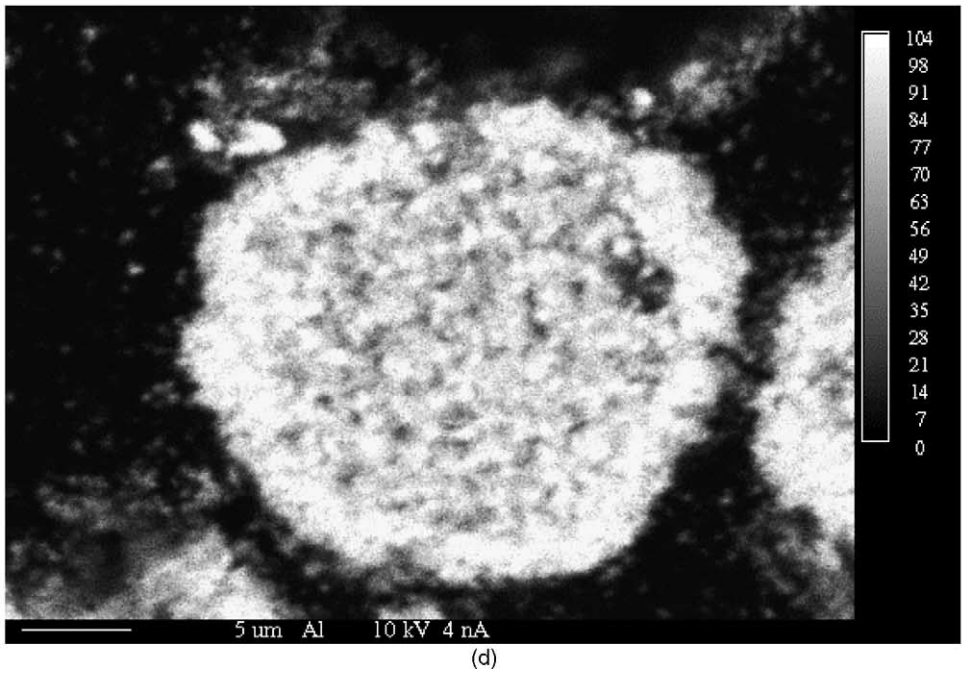

(d)

Fig. 5. (*Continued*).

In order to assess the phase distributions which might be expected from such reactions the phase diagram (plotted in atomic concentration) shown in Fig. 6 has been assembled. It is necessary to plot in this way rather than the more usual oxide compositions in order to take account of the variable valency of zirconium between ZrO and ZrO_2. The diagram shows the stoichiometric composition which is given by the reaction

$$2Al + 3ZrO_2 \rightarrow Al_2O_3 + 3ZrO \quad (1)$$

and which corresponds to an aluminium concentration in the reactant mix of 12.7 w/o. Thus, the present experiments with 20 w/o Al have an excess of metal for this reaction (E_o). Further, from the X-ray diffraction results (E_s) the products of reaction lie within the triangle ZrO–ZrO_2–Al_2O_3.

There is, therefore, an inconsistency between the starting and final phase compositions thus defined and which can be explained either by the system having failed to reach equilibrium during the reaction (which is unlikely) or by a net increase in the amount of oxygen in the reaction system given

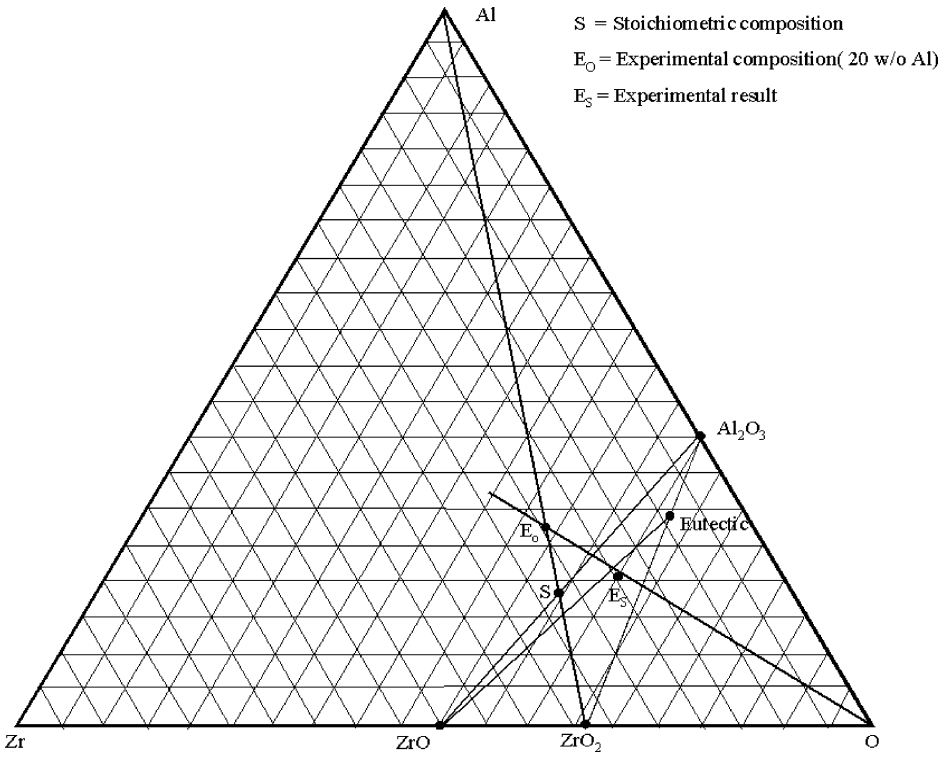

Fig. 6. Ternary composition diagram of the Zr–Al–O system (atomic concentration).

by Eq. (1). The latter effect can be represented either as a chemical reaction or by plotting on the ternary phase diagram. The latter is achieved by taking quantified diffraction data for the proportions of phases from a sample of composition 20Z sintered at 1500 °C (Tables 1 and 2, Fig. 6) which has the phase composition 46 w/o ZrO, 33 w/o Al_2O_3 and 21 w/o ZrO_2 and plotting this (in appropriate composition units) on Fig. 6 (E_s). The change in oxygen concentration from the starting to the final composition is given by the distance E_oE_s on the diagram (Fig. 6). It is assumed that there is no gain or loss of the metallic elements and this is confirmed by the extrapolation of E_oE_s, which passes through the oxygen (O) corner of the diagram. The increase in oxygen content during sintering is from 49.6 at.% (21.6 wt.%) in the starting mixture to 59.4 at.% (28.8 wt.%) in the sintered sample and this is assumed to come from oxygen in the sintering (hot-pressing) atmosphere. The equivalent chemical reaction (equivalent to the point E_s in Fig. 6) is then

$$2Al{+}2ZrO_2 + 0.8O_2 \rightarrow Al_2O_3 + 1.4ZrO + 0.6ZrO_2 \quad (2)$$

(given the accuracy of determination of the phase composition by diffraction and hence the precision of point E_s, Eq. (2) has been rounded to the first decimal place of numbers of moles). In principal, from such an equation an oxygen partial pressure could be calculated for reaction of the pure phases and which could then be compared to the expected p_{O_2} for the sintering system. However, no data is available for the free energy of formation of ZrO and so the calculation cannot be done in that way. Conversely, if a value of p_{O_2} is calculated for the hot-pressing conditions used in these experiments then an estimate of the stability of ZrO can be made as follows.

The hot-press system consists of carbon tooling which at the start of the experiment is in air ($21\%O_2 + 79\%N_2$). On heating it is assumed that all of the oxygen contained in the heated enclosure is converted at 1500 °C to carbon monoxide

$$2C + O_2 \rightarrow 2CO \quad (3)$$

and thus 2 mol of CO are created from every mole of oxygen with the nitrogen remaining unchanged. The relative partial pressures are then (assuming the heated enclosure to be a closed system)

$$p_{CO} = 0.35\,\text{atm} \qquad p_{N_2} = 0.65\,\text{atm}$$

The equivalent partial pressure of oxygen can then be calculated from Eq. (3) and the free energy of formation of carbon monoxide[9]

$$p_{O_2} = 2.2 \times 10^{-17}\,\text{atm}$$

Putting this value into Eq. (2) and using the relevant free energy data for that set of compounds in their pure state[9] the free energy of formation of ZrO at 1500 °C is

$$\Delta G_O(\text{ZrO}) = -294,500\,\text{J mol}^{-1}\ (-70,460\,\text{cal mol}^{-1})$$

This value is consistent with the values of free energy of formation of the corresponding carbide and nitride of zirconium and with that of other transition metal carbide, nitride and monoxide series.[9]

The above analysis of Fig. 6 and Eq. (2) gives the overall changes which result from the experimental conditions used. However, it does not provide a mechanism by which the reaction takes place and by which the observed microstructure forms; this is somewhat more speculative.

It may reasonably be assumed that just as the oxygen pressure in the sintering system is controlled by the external gas atmosphere, so the number of moles of oxygen in addition to those in the zirconia starting compound (Eq. (2)) arise from gas (air) within the compact pellet. As the temperature rises and metallic aluminium melts then reaction with the gas takes place to form a thin skin of aluminium oxide around the metal particles. This is exothermic but at this stage is limited in extent. It is known from thermal analysis data[6] that a marked exotherm occurs at about 1000 °C when the major reaction of aluminium metal occurs with residual gas and, more importantly, above 1200 °C in the reduction of the zirconia ceramic powder matrix. As this strongly exothermic reaction proceeds both zirconium and oxygen are incorporated locally in metal particles to form Al–Zr–O mixed oxide phases which when cooled are seen as the Al_2O_3–ZrO_2 "eutectic" structure of Fig. 4. Although the areas corresponding to the prior metal particles have a eutectic oxide appearance and the phase composition is consistent with this (Fig. 6) it would require temperatures locally in excess of 1710 °C to form a true eutectic.[10] The strongly reducing action of the aluminothermic reaction reduces the matrix of zirconia grains to the monoxide (ZrO) phase which is confirmed by X-ray diffraction (Fig. 1) as the major phase. It is emphasised that these deductions are speculative but they are consistent with the diffraction and microstructural evidence.

5. Conclusions

It has been shown that the aluminothermic reduction of zirconia can be used to produce composite microstructures with a heterogeneous distribution of phases. Under suitably reducing conditions the principal phase is zirconium monoxide which is formed together with alumina and cubic zirconia. The results show that reaction of aluminium metal with zirconia powder proceeds with incorporation of oxygen from the sintering gas at low partial pressure and that both zirconium and oxygen are incorporated into the former aluminium particles as reaction proceeds. The resulting microstructure is consistent with a mechanism in which dissolution of zirconium and oxygen in the (liquid) metal at sintering temperatures leads to formation of a reduced matrix of zirconium monoxide.

The free energy of formation of zirconium monoxide has been estimated as $-294{,}500\,\mathrm{J\,mol^{-1}}$ which is consistent with the values for similar transition metal monoxides. The structure of ZrO is a rock-salt cubic unit-cell and the unit-cell dimension is 0.46258 nm.

References

1. Stevens, R., *An Introduction to Zirconia. MEL Publication No 113*. Magnesium Elektron, Manchester, UK, 1983.
2. Butler, E. P., Transformation toughened zirconia ceramics. *Mater. Sci. Tech.* 1985, **1**, 417.
3. Singh, J. R., Poeppel, R. B., James, J. J. and Picciolo, J. J., Microstructural development of refractory composites with improved fracture toughness. In *Microstructure and Properties of Refractories, Key Engineering Materials, Vol 88*, ed. J. R. Singh and S. Banerjee. Trans Tech Publications, Aedermansdorf, Switzerland, 1993, p. 103.
4. Zhe, X. and Hendry, A., In situ synthesis of hard and conductive ceramic composites from Al and ZrO_2 mixtures by reaction hot pressing. *J. Mater. Sci. Lett.* 1998, **17**, 687.
5. Zhe, X., Watson, L. M. and Hendry, A., Formation of meta-stable zirconium monoxide during thermite reaction hot pressing. In *Proceedings of 4th International Conference on SHS*, ed. M. A. Rodriguez. ICV, Madrid, Spain, 1997.
6. Zhe, X., *Novel Zirconium Oxide-based Ceramic Composites*. Ph.D. thesis, University of Strathclyde, 1999.
7. Liddell, K., University of Newcastle Upon Tyne, unpublished work, 1996.
8. Aschermann, R. J., Garg, S. P. and Rauh, E. G., High temperature phase diagram of the system Zr–O. *J. Am. Ceram. Soc*. 1977, **60**, 341.
9. Kubaschewski, O. A., *Metallurgical Thermochemistry*. Pergamon Press, London, 1979.
10. *Phase Diagrams for Ceramists (Figure 4377)*, ed. E. M. Levin and H. F. McMurdie. American Ceramic Society, Columbus, OH, USA, 1975.